SCIENCE CHINA
Chemistry

• ARTICLES •
• SPECIAL TOPIC • The Frontiers of Chemical Biology and Synthesis

January 2012 Vol.55 No.1: 70–79
doi: 10.1007/s11426-011-4465-x

Synthesis, physicochemical and biological properties of oligonucleotides incorporated with amino-isonucleosides

WANG Fang†, CHEN Yue†, HUANG Ye, JIN Hong-Wei, ZHANG Liang-Ren, YANG Zhen-Jun* & ZHANG Li-He

State Key Laboratory of Natural and Biomimetic Drugs; School of Pharmaceutical Sciences, Peking University, Beijing 100191, China

Received August 30, 2011; accepted October 10, 2011; published online December 2, 2011

Antisense oligonucleotides (ASONs) and siRNAs have been applied extensively for the regulation of cellular and viral gene expression, and RNAi is currently one of the most promising new approaches for anti-tumor and anti-viral therapy. In order to improve bioactivity properties and physicochemical properties of siRNA, we synthesized a novel class of ASONs **II–VII** incorporated with amino-isonucleoside (**isoA$_1$** and **isoA$_2$**) for investigation on basic physicochemical properties. Then we designed amino-isonucleoside (**isoA$_1$, isoA$_2$** and **isoT$_1$**) incorporated siRNA **2–7**. Some meaningful results have been obtained from the physicochemical property experiments in ASONs. In RNAi potency experiments, we investigated RNAi potency of each strand of the siRNA. These amino-isonucleosides incorporated siRNAs showed promising bioactivity properties and had position specificity. Reduced off target effect from sense strand loading in siRNA application was observed.

amino-isonucleoside, antisense oligonucleotide, siRNA

1 Introduction

Oligonucleotides, such as antisense oligonucleotides (ASONs) and siRNAs have been applied extensively for the regulation of cellular and viral gene expression, and RNAi technology is becoming one of the most promising new approaches for the therapy of many irremediable diseases [1–3]. Both ASONs and siRNAs take action by hybridizing to mRNA targets by Watson-Crick base pairing and inhibit translation of mRNA in a sequence-specific manner [2, 4]. Native oligonucleotide shows low enzymatic stability and cellular permeability [5, 6]. There are many problems associated with the effective use of siRNA for *in vivo* application, such as off-target effects, cytotoxicity, and poor pharmacokinetic properties [7]. Chemical synthesis of siRNA using phosphoramidite building blocks to produce single-stranded oligonucleotides followed by annealing to form duplexes is a generally accepted approach in this research [8]. This approach permits incorporation of a wide variety of natural and artificial modifications into the siRNA that can help solve some of the problems associated with administration of synthetic nucleic acids into cells or animals [9].

Isonucleosides represent a novel class of carbohydrate-modified nucleoside in which the nucleobase is linked to various positions of ribose other than C-1′, and some of these nucleosides have shown interesting biological activities [10–14]. In our previous reports regarding the synthesis and incorporation of isonucleosides into antisense oligonucleotides, we found that modification of the terminal group confers strong nuclease resistance, while modification in the central region of the antisense oligonucleotide with L-isonucleoside enables it to become good substrates of RNase H [15]. Introduction of an amino group into the isonucleoside may form a Zwitterionic molecule, and increase the thermal stability of the isonucleoside-modified oligonucleotide with its complementary sequence. This is because in the physio-

*Corresponding author (email: yangzj@bjmu.edu.cn)
†These authors contributed equally to this work

logical conditions, the positively charged amino moiety should interact with the negatively charged phosphate backbone more strongly than the uncharged hydroxyl group [16]. To be used as a probe, the amino group can also be attached with a fluorescent group such as pyrene to monitor RNA folding [17]. We had reported the amino-isonucleoside **isoA$_1$** (Figure 1) incorporated siRNA (related to 3′ end of the coding sequence of the wee1 mRNA), and found that amino-isonucleoside modification at the 3′ or 5′ terminal of sense strand showed less effects on RNA duplex thermal and serum stabilities, and their functional activities are also comparable to their native siRNAs. However, the modification on the antisense strand at the corresponding positions showed a dramatic negative RNAi potency [18].

Here, we investigate the physicochemical and biological properties of the amino-isonucleoside (**isoA$_1$** and **isoA$_2$**) modified oligonucleotides and add another kind of amino-isonucleoside structure which has an elongated amino side chain to assist the analysis of influence of amino-isonucleoside modification on the oligonucleotides. Upon incorporating more than one isonucleosides on the same oligonucleotides strand, the formation of duplex would be blocked by the tortuosity of L-isonucleoside. For this reason, we incorporate only one amino-isonucleoside at a time in this study. Modifications of the sense strand were reported to be tolerated and the cleavage site (10–11th) and seed region (2nd–8th) of antisense strand have been proved to be important for the retainment of siRNA silence activity. Considering the importance of the middle site and the two terminals for the oligonucleotides, we design the amino-isonucleoside modified antisense oligonucleotides **II–VII** and amino-isonucleoside modified siRNAs **2–7**. We analyzed the physicochemical properties of such modifications at different positions of ASONs and further investigated the RNAi potency of each strand of the modified siRNAs (related to cyclin B1-complexed CDC2). These results will be useful in the choice of modified strategies.

2 Materials and method

2.1 General

All solvents were dried and distilled prior to use. Chemical reagents were purchased from Acros and Sigma Co. Thin layer chromatography was performed on silica gel GF-254 (Qing-Dao Chemical Co., China) plates with detection by UV or by heating. Silica gel (200–300 mesh; Qing-Dao Chemical Co.) was used for short column chromatography. NMR spectra were recorded on a Varian VXR-300 and Varian Inova-500 instrument. ^{1}H NMR spectra were referenced using internal standard TMS and ^{31}P NMR spectra using external standard 85% H_3PO_4. Mass spectra (ESI-TOF$^+$ MS) and high resolution mass spectra (ESI-TOF$^+$ HRMS) were obtained on MDS SCIEX QSTAR and Bruker DALTONICS APEX IV 70e instruments. MALDI-TOF mass spectra for oligonucleotides were obtained at SIMADZU AXIMA CFR plus, and the data are reported in *m/e* (intensity to 100%).

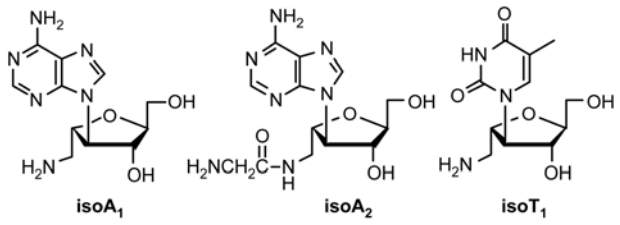

Figure 1 Structure of **isoA$_1$**, **isoA$_2$** and **isoT$_1$**.

2.2 Synthesis of amino-isonucleoside phosphoramidites

*4-Deoxy-4-(adenin-9-yl)-6-deoxy-6-(N-tert-butyloxycarbonyl-glycin)-amino-2,5-anhydro-L-mannitol (**4**)*

To a mixture of N-(Boc)glycine (0.95 g, 5.41 mmol) and DCC (1.29 g, 6.25 mmol) in CH_2Cl_2 (10 mL) were added **isoA$_1$** (1.167 g, 4.16 mmol) and *N,N*-diisopropylethylamine (0.84 mL, 4.16 mmol) in anhydrous DMF (10 mL). The resulting mixture was stirred at room temperature for 48 h and was concentrated under reduced pressure. The residue obtained was purified by silica gel column chromatography (10:1 dichloromethane/methanol, 0.5% $NH_3{\cdot}H_2O$) to yield compound **4** (0.751 g, recovery yield 63.6%).

^{1}H NMR (500 MHz, DMSO-d_6): 1.37 (s, 9H, Boc), 3.23–3.26 (t, 2H, H-6a, H-6b), 3.49–3.51 (t, 2H, BocNHCH$_2$), 3.54–3.59 (m, 1H, H-1a), 3.64–3.68 (m, 1H, H-1b), 3.81–3.84 (m, 1H, H-2), 4.44–4.47 (m, 1H, H-5), 4.50–4.54 (t, 1H, H-4), 4.73–4.77 (m, 1H, H-3), 4.84–4.86 (t,1H,1-OH), 5.61–5.62 (d, 1H, 3-OH), 6.90–6.92 (t, 1H, BocNH), 7.99 (t, 1 H, 6-NH); For adenin-9-yl: 7.24 (s, 2H, –NH$_2$), 8.08 (s, 1H, H-8), 8.14 (s, 1H, H-2). ^{13}C NMR (125 MHz, DMSO-d_6): 28.2 (Boc), 40.3 (C-6), 43.1 (BocNHCH$_2$), 61.4 (C-1), 64.0 (C-4), 72.8 (C-3), 76.9 (C-5), 78.0 (Boc), 83.3 (C-2), 155.8 (Boc), 169.7 (6-CO); For adenin-9-yl: 119.4 (C-5), 140.7 (C-8), 149.4 (C-4), 152.3 (C-2), 156.1 (C-6). HRMS (ESI-TOF)$^+$: Anal. calcd for $C_{18}H_{27}N_7O_6$ (M+H, Na)$^+$ 438.2096, 460.1915; found: 438.2099, 460.1917.

*4-Deoxy-4-(6-benzoylamino-purin-9-yl)-6-deoxy-6-(N-tert-butyloxy carbonylglycin)-amino-2,5-anhydro-L-mannitol (**5**)*

Compound **4** (1.10g, 2.51 mmol) was dissolved in dry pyridine (20 mL). TMSCl (3.8 mL, 25.11 mmol) was added at 0 °C. The resulting solution was stirred at room temperature for 3 h. Benzoyl chloride (1.93 mL, 15.07 mmol) was added at 0 °C and the solution was stirred at room temperature for 3 h. The pH of the solution was adjusted to 8–9 by $NH_3 \cdot H_2O$ at 0 °C. The solution was stirred at room temperature for 1 h. After evaporation, the mixture was dissolved in CH_2Cl_2 (50 mL). After filtration, the solvent was evaporated under vacuum and the residue was purified by silica gel

column chromatography (18:1 dichloromethane/methanol, 0.2% $NH_3 \cdot H_2O$) to yield **5** (1.08 g, 79.4%).

^{1}H NMR (500 MHz, $CDCl_3$): 1.39 (s, 9H, Boc), 3.40 (br s, 1H, H-6a), 3.53 (br s, 1H, H-6b), 3.76 (d, 2H, BocNH-CH_2), 3.85 (br s, 2H, H-1a, H-1b), 4.05–4.14 (br s, 2H, H-2, H-5), 4.66 (s, 1H, H-4), 5.06 (br s, 1H, H-3), 5.38 (br s, 1H, 1-OH), 5.65(br s, 1H, 3-OH), 7.14 (br s, 1H, BocNH), 7.45–7.48 (t, 2H, Ph), 7.54–7.57 (t, 1H, Ph), 7.96–7.98 (d, 2H, Ph); For adenin-9-yl: 8.15 (s, 1H, H-8), 8.53 (s, 1H, H-2), 9.48 (br s, 1H, NHCOPh). ^{13}C NMR (125 MHz, $CDCl_3$): 28.3 (Boc), 40.4 (C-6), 44.4 (BocNHCH_2), 62.1 (C-1), 65.3 (C-4), 73.8 (C-3), 77.7 (C-5), 80.5 (Boc), 83.5 (C-2), 128.0, 128.8, 132.9, 133.2 (Ph), 151.9 (Boc), 171.1 (6-CO); For adenin-9-yl: 123.1 (C-5), 144.0 (C-8), 149.3 (C-4), 151.5 (C-2), 156.5 (C-6), 165.2 (NHCOPh). MS (ESI-TOF)$^+$: *m/z* 542 $(M+H)^+$, 564$(M+Na)^+$. Anal. calcd for $C_{25}H_{31}N_7O_7$ (541.23): C, 55.45; H, 5.77; N, 18.10. Found: C, 55.19; H, 6.14; N, 17.35.

*4-Deoxy-4-(6-benzoylamino-purin-9-yl)-6-deoxy-6-(N-trifluoroacetyl-glycin)-amino-2,5-anhydro-L-mannitol (**6**)*

Compound **5** (0.82 g, 1.52 mmol) was dissolved in 3 M HCl-EtOAc (60 mL). The mixture was stirred for 4 h and neutralized by NaOH. Then the solution was concentrated in vacuo and the mixture was dissolved in EtOH (40 mL). After filtration, the solvent was evaporated under vacuum to yield the crude compound 4-deoxy-4-(6-benzoylamino-purin-9-yl)-6-deoxy-6-(*N*-glycin)-amino-2,5-anhydro-L-mannitol (**6–1**). Et_3N (1.34 mL, 9.12 mmol) and ethyl trifluoroacetate (0.83 mL, 6.1 mmol) were added dropwise to the mixture of compound **6–1** (0.67 g, 1.52 mmol) and CH_3OH (20 mL) in an ice bath. The mixture was stirred overnight at room temperature. After evaporation, the residue was purified by silica gel chromatography (10:1 dichloromethane/methanol, 0.2% Et_3N) to yield **6** (0.79 g, colorless syrup) in 97.5% yield.

^{1}H NMR (500 MHz, DMSO-d_6): 3.26–3.29 (m, 2H, H-6a, H-6b), 3.58–3.63 (m, 1H, H-1a), 3.68–3.72 (m, 1H, H-1b), 3.78–3.80 (m, 2H, TFANHCH_2), 3.87–3.90 (m, 1H, H-2), 4.54–4.58 (m, 1H, H-5), 4.68–4.72 (t, 1H, H-4), 4.78–4.83 (m, 1H, H-3), 4.88–4.91 (t, 1H, 1-OH), 5.73 (d, 1H, 3-OH), 7.54–7.57 (t, 2H, Ph), 7.64–7.67 (t, 1H, Ph), 8.04–8.06 (d, 2H, Ph), 8.33–8.35 (t, 1H, 6-NH), 9.59–9.61 (t, 1H, NHCOCF_3); For adenin-9-yl: 8.43(s, 1H, H-8), 8.75 (s, 1H, H-2), 11.17 (s, 1H, NHCOPh). ^{13}C NMR (125 MHz, DMSO-d_6): 40.5 (C-6), 41.7 (TFANHCH_2), 61.3 (C-1), 64.2 (C-4), 72.9 (C-3), 76.7(C-5), 83.2 (C-2), 128.4, 132.4, 133.4 (Ph), 156.5, 156.8 (CF_3CO), 167.4 (6-CO); For adenin-9-yl: 126.0 (C-5), 144.3 (C-8), 150.3 (C-4), 151.3 (C-2), 152.3 (C-6), 165.6 (NHCOPh). MS (ESI-TOF)$^+$: *m/z* 538 $(M+H)^+$, 560 $(M+Na)^+$. HRMS (ESI-TOF)$^+$: Anal. calcd for $C_{22}H_{22}N_7O_6F_3$ $(M+H, Na, or K)^+$ 538.1656, 560.1476, 576.1215; Found: 538.1658, 560.1478, 576.1221.

*1-O-(4,4'-Dimethoxytrityl)-4-deoxy-4-(6-benzoylamino-purin-9-yl)-6-deoxy-6-(N-trifluoroacetyl glycin)-amino-2,5-anhydro-L-mannitol (**7**)*

Dimethoxytrityl (DMT) chloride (636 mg, 1.88 mmol) was added to the mixture of compound **6** (672 mg, 1.25 mmol) in dry pyridine (30 mL) at 0 °C. The resulting solution was stirred at room temperature for 48 h. After evaporation, the residue was purified by a short-column chromatography (25:1 dichloromethane/methanol, 0.2% Et_3N) to yield **7** (562 mg, 53.5%).

^{1}H NMR (500 MHz, DMSO-d_6): 3.16–3.42 (m, 4H, H-1a, H-1b, H-6a, H-6b), 3.75 (s, 6H, PhOCH_3), 3.78–3.87 (m, 2H, TFANHCH_2), 4.05–4.08 (m, 1H, H-2), 4.66–4.75 (m, 2H, H-4, H-5), 4.97–5.02 (m, 1H, H-3), 5.75 (d, 1H, 3-OH), 6.91–8.06 (m, 18H, Ph), 8.42–8.44 (t, 1H, 6-NH), 9.61 (br s, 1H, NHCO–CF_3); For adenin-9-yl: 8.37(s, 1H, H-8), 8.73(s, 1H, H-2), 11.16 (br s, 1 H, NHCOPh). ^{13}C NMR (125 MHz, DMSO-d_6): 40.2 (C-6), 41.8 (TFANHCH_2), 55.0 (PhOCH_3), 63.7 (C-1), 64.1 (C-4), 72.5 (C-3), 76.2 (C-5), 81.1 (C-2), 85.3 (Ph_3C), 113.2, 126.2, 126.6, 127.8, 128.4, 129.8, 132.4, 133.4, 135.7 (Ph), 158.0 (CF_3CO), 167.5 (6-CO); For adenin-9-yl: 144.7 (C-5), 145.0 (C-8), 150.4 (C-4), 151.2 (C-2), 152.3 (C-6). MS (ESI-TOF)$^+$: *m/z* 840 $(M+H)^+$, 862 $(M+Na)^+$. HRMS (ESI-TOF)$^+$: Anal. calcd for $C_{43}H_{40}N_7O_8F_3$ $(M+H, Na, K)^+$ 840.2963, 862.2783, 878.2522; Found: 840.2966, 862.2785, 878.2520.

*1-O-(4,4'-Dimethoxytrityl)-3-O-(2-cyanoethyl-N,N-diisopropyl)phosphoramidite-4-deoxy-4-(6-benzoylamino-purin-9-yl)-6-deoxy-6-(N-trifluoroacetyl-glycin)-amino-2,5-anhydro-L-mannitol (**2**)*

Compound **7** (380 mg, 0.453 mmol) and 1-*H*-tetrazole (42 mg, 0.602 mmol) were dissolved in anhydrous CH_2Cl_2 (10 mL) under argon atmosphere. The mixture was stirred at room temperature for about 15 min, 2-cyanoethyl-*N,N,N',N'*-tetraisopropyl-phosphoramidite (0.19 mL, 0.590 mmol) was added dropwise, and the reaction mixture was stirred for 3 h. TLC analysis (50:50 CH_2Cl_2/EtOAc) indicated completion of the reaction. The reaction mixture was then diluted with CH_2Cl_2 (20 mL), extracted with 5% $NaHCO_3$ solution (15 mL × 2), washed with brine (20 mL x 2), and dried over Na_2SO_4. Evaporation to dryness yielded a white foam, which was dissolved in CH_2Cl_2 (3 mL), and applied to a silica gel column equilibrated with CH_2Cl_2 containing 0.5% Et_3N. Elution with CH_2Cl_2/EtOAc (1:1–1:1.6, 0.5% Et_3N) yielded **2** (291 mg, 61.0%) as a white foam.

^{31}P NMR (121.50 MHz, DMSO-d_6): 149.63 and 150.32 (d).

2.3 Synthesis of the amino-isonucleoside modified oligonucleotides

The amino-isonucleoside modified oligonucleotides were prepared by solid phase phosphoramidite chemistry (DMT

on) using an Applied Biosystems 381A DNA synthesizer. For the purpose of operation convenience, the synthesis was started with the commercially available controlled pore glass (CPG) with cytidine-loaded. The 0.1 M solution of amidites **1** and **2** in anhydrous acetonitrile was used for the synthesis of the modified oligonucleotides. For incorporation of **1** and **2**, the phosphoramidite solutions were delivered in three portions, each followed by a 10 min coupling wait time. All other steps in the protocol provided by Applied Biosystems were used without modifications. After completion of the synthesis, CPG was suspended in aqueous ammonium hydroxide (30 wt%) and kept at 55 °C overnight to complete the removal of all protecting groups. The CPG was filtered and the crude oligonucleotides were purified by high performance liquid chromatography (HPLC, C-18, A = 50 mM triethyl-ammonium bicarbonate, pH 7.0, B = acetonitrile, 0 to 40% B in 40 or 50 min, flow rate 5.0 mL/min, λ = 260 nm). Detritylation with aqueous acetic acid (80%) followed by desalting (Sephadex G-25) gave crude oligonucleotides **II–VII**. The crude oligomers were further purified by HPLC (ZORBAX Bio Series Oligo Column, 6.2 mm ID × 80 mm), with gradient eluting using eluants A (MeCN/ 0.02 M NaH_2PO_4, 1:4) and B (1.0 M NaCl in A) at 1.0 mL/min flow rate. The fractions containing pure oligonucleotides were desalted by a Sephadex G-25 column. The pure oligonucleotides were lyophilized and stored at −20 °C. Other natural oligonucleotides were purchased from TaKaRa Biotechnology (Dalian) Co., Ltd.

2.4 UV melting experiments

Determination of the T_m of the ASON/DNA hybrids was carried out in the following buffer: 57 mM Tris-HCl (pH 7.5), 57 mM KCl, 1 mM $MgCl_2$. Absorbance was monitored at 260 nm in the temperature range from 20 to 80 °C using a UV-visible spectrophotometer with the heating rate of 0.5 °C per minute. Prior to measurements, the samples (0.85 μM of ASON and 0.75 μM of DNA mixture) were preannealed by heating to 90 °C for 5 min followed by slow cooling to 4 °C and keeping this temperature overnight.

2.5 CD spectra

CD Spectra were recorded from 300 to 200 nm in 1 cm path length cuvettes. Spectra were obtained with an ASON/DNA duplex concentration of 0.75 μM in buffer containing 57 mM Tris-HCl (pH 7.5), 57 mM KCl and 1 mM $MgCl_2$. All the spectra were measured at 20 °C with a *J*715 CD spectrophotometer (*JAC*).

2.6 Exonuclease degradation studies

Stability of the ASONs toward 3′-exonuclease was tested using snake-venom phosphodiesterase (SVPDE). All reactions were performed at 7.1 μM DNA concentration in 56 mM Tris-HCl (pH 7.9) and 4.4 mM $MgCl_2$ at 37 °C. Exonuclease concentration of 28.6 ng/μL was used for digestion of oligonucleotides. The total reaction volume was 14 μL. Aliquots were taken at 0, 10, 20, 40, 60 min and quenched by addition of the same volume of 50 mM EDTA in 95% formamide. Reaction progress was monitored by 20% denaturing (7 M urea) PAGE and was visualized by staining with SYBR gold and quantified by Model & Storm 860 hardware and Imagequant software (Amersham Biosciences, PKU, China).

2.7 Endonuclease degradation studies

Stability of ASONs toward endonuclease was tested using DNase I from bovine pancreas. Reactions were carried out at 10 μM DNA concentration in 100 mM Tris-HCl (pH 7.5) and 10 mM $MgCl_2$ at 37 °C using 15 unit of DNase I. The total reaction volume was 10 μL. Aliquots were taken at 0, 2, 4, 10, 20, 40 and 60 min and quenched with the same volume of 50 mM EDTA in 95% formamide, which were resolved in 20% polyacrylamide, respectively, then applying in denaturing (7 M urea) gel electrophoresis. The analytic results were visualized by staining with SYBR gold and quantified by Model & Storm 860 hardware and Imagequant software (Amersham Biosciences, PKU, China).

2.8 Computer simulation

All Molecular dynamics (MD) simulations were performed with the AMBER 8 molecular simulation package. The AMBER 99 force field was used to describe the DNA:RNA. Starting models of the studied DNA:RNA duplexes were built in the A canonical structures using the Insight II package. All constructed oligonucleotide duplexes were solvated in TIP3P water using a rectangular box, which extended 10 Å away from any solute atom. To neutralize the negative charges of simulated molecules, Na^+ counterions were placed next to each phosphate group. Molecular dynamics (MD) simulations were carried out using the SANDER module of AMBER 8. The production simulations of 2.0 ns for all duplexes were performed at constant pressure (1 atm) and temperature (300 K). The final structure of each duplex was produced from 1000 steps of the minimized averaged structure of the last 1.5 ns of MD. Free-energy analysis was performed using the MM_PBSA scripts supplied by AMBER 8.

2.9 Cell culture

HEK293 cell line was obtained from Dr. Zicai Liang (LNAT, IMM, PKU). The HEK293 cell line was cultured in DMEM (Hyclon, USA) supplemented with 10% FBS, 50 IU/mL penicillin, and 50 μg/mL streptomycin at 37 °C in a humidified atmosphere containing 5% CO_2.

2.10 RNAi potency assay

Oligonucleotides and plasmids in RNAi assay: DNA oligonucleotides were from Invitrogen (Beijing, China). Normal RNA oligonucleotides were from Genepharma (Shanghai, China). Plasmid DNAs were extracted using a mini-purification kit (Promega). siQuant vector was a gift from Institute of Molecular Medicine, Peking University, Beijing.

Human embryonic kidney (HEK293) cells were grown in Dulbecco's modified Eagle's medium supplemented with 10% fetal bovine serum, 2 mM L-glutamine, 100 U/mL penicillin and 100 mg/mL streptomycin (Life Technologies, Gibco). The cells were seeded into 24-well plates at a density of ~1 × 10^5 cells/well one day before transfection. siQuant vector (0.17 mg/well) carrying the target site of tested siRNA was transfected into HEK293 cells at approximately 50% confluence, together with pRL-TK control vector (0.017 mg/well), with or without the siRNA (16.7 nM). The activities of both luciferases were determined by a fluorometer (Synergy HT, BioTek, USA) before the firefly luciferase activity was normalized to renilla luciferase for each well. Silencing efficiency of each siRNA was calculated by comparison with a sample without siRNA treatment. All experiments were performed in triplicate and repeated at least twice.

3 Results and discussion

3.1 Synthesis of building blocks 1, 2 and 3 for $isoA_1$, $isoA_2$ and $isoT_1$

The building blocks **1** and **3** (Figure 2) for $\mathbf{isoA_1}$ and $\mathbf{isoT_1}$ were synthesized following the previously reported protocol by Li *et al*. [18]. For the building block **2** of $\mathbf{isoA_2}$ which has a longer side chain containing an amino group, the synthetic route was altered to include glycylation of 6-amino group, which requires a different protecting group of the glycol (Scheme 1).

3.2 Synthesis of oligonucleotides II–VII

Oligodeoxynucleotide synthesis was carried out at the 1 μmol scale using Applied Biosystem model 381 DNA Synthesizer according to regular phosphoramidite chemistry created by Caruthers. At the modified position, the native phosphoramidites (0.12 M) were replaced by corresponding amino-isonucleoside phosphoramidites building blocks **1** and **2** (0.1 M), respectively, characterized. The isolated yields (by anion exchange high-performance liquid chromatography) of modified oligonucleotides (**II–VII**) were 30%–40%, which are similar to those during unmodified DNA oligomer synthesis. The products were characterized by MALDI-TOF mass spectroscopy (Table 1).

3.3 Synthesis of siRNA single strand A or B

According to the standard procedure for the synthesis of single strand of RNA oligomer, the native phosphoramidites (0.12 M) were respectively replaced by corresponding amino-isonucleoside phosphoramidites building blocks **1**, **2** and **3** (0.1 M) at the modified step. Furthermore, an extended coupling time of 900 second was used to replace the standard coupling time of 600 second used for the native phosphoramidites (rA^{Bz}、 rG^{Ac}, rC^{Ac}, rU) due to the steric effect of modified phosphoramidites. The crude product was purified by anion exchange high-performance liquid chromatography and characterized by MALDI-TOF mass spectroscopy (Table 2).

3.4 Binding ability to complementary single strand DNA or RNA

The thermal stability of duplexes involving $\mathbf{isoA_1}$ and $\mathbf{isoA_2}$ was examined by hybridization properties of oligonucleotides **I–VII** with complementary DNA **VIII** as shown in Table 3. The results revealed that all oligomers **II–VII** succeeded in hybridizing with **VIII** to form stable duplexes. When $\mathbf{isoA_1}$ and $\mathbf{isoA_2}$ were incorporated in the center of oligomers (**IV** and **VI**), the T_m values were decreased by 5.8 and 7.9 °C, respectively, when compared with their natural counterpart. When $\mathbf{isoA_1}$ and $\mathbf{isoA_2}$ were appended to the 3′-end of oligomers (**III** and **VII**), the T_m values were decreased by 3.9 and 5.0 °C, respectively. When $\mathbf{isoA_1}$ and $\mathbf{isoA_2}$ were appended to the 5'-end of oligomers (**II** and **V**), the T_m values were decreased by 3.9 and 4.9 °C, respectively. The reason of such thermal stability decreasing is that the

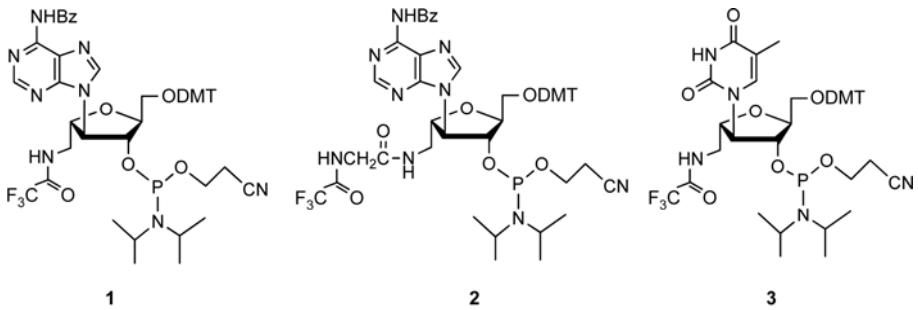

Figure 2 Structures of building blocks **1**, **2** and **3**.

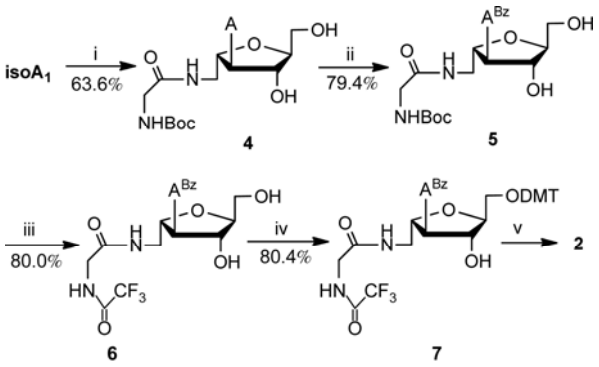

Scheme 1 Synthesis of building block **2**. Reagents and conditions: i) $BocNHCH_2COOH$, DCC, DIPEA; ii) TMSCl, BzCl, Py; iii) a. 3 M HCl-EtOAc; b. $CF_3COOC_2H_5$, Et_3N, CH_3OH; iv) DMTrCl, Py; v) 1-H-tetrazole, 2-cyanoethyl-*N,N,N',N'*-tetraisopropyl-phosphoramidite.

formation of Watson-Crick hydrogen bonding was perturbed by the torsion of the backbone at the position of modification. Also, the thermal stability results of the duplexes involving **isoA$_1$** and **isoA$_2$** with complementary RNA **IX** are shown in Table 3, demonstrating that the T_m values of the modified ones were decreasing when compared with their natural counterpart. Especially, the **isoA$_2$** incorporated ones (**V**, **VI**, and **VII**) show less influence than the **isoA$_1$** incorporated ones (**II**, **III** and **IV**). But this trend was not obvious in the DNA/DNA duplex. The structure of DNA/RNA duplex (T_m = 76.0 °C) is more compact than the DNA/DNA (68.0 °C) because of the 2′-hydroxyl group of RNA. The difference between **isoA$_1$** and **isoA$_2$** modification may be due to the release of the torsion strain of duplex in the long side chain of amide in **isoA$_2$**.

Table 1 Modification on ASONs by **isoA$_1$** and **isoA$_2$** incorporation

No.	Modification on ASON	MALDI-TOF MS (calcd)	MALDI-TOF MS (found)
I	5′-ACATCTCCCGCATCCCACTC-3′		
II	5′-AC***isoA$_1$***TCTCCCGCATCCCACTC-3′	5933	5933
III	5′-ACATCTCCCGCATCCC***isoA$_1$***CTC-3′	5933	5932
IV	5′-ACATCTCCCGC***isoA$_1$***TCCCACTC-3′	5933	5933
V	5′-AC***isoA$_2$***TCTCCCGCATCCCACTC-3′	5990	5993
VI	5′-ACATCTCCCGC***isoA$_2$***TCCCACTC-3′	5990	5993
VII	5′-ACATCTCCCGCATCCC***isoA$_2$***CTC-3′	5990	5993
c-DNA (**VIII**)	3′-TGTAGAGGGCGTAGGGTGAG-5′		

Table 2 Modified **siCdc-2** by **isoA$_1$**, **isoA$_2$** and **isoT$_1$** incorporation

No	Modification on single strands of **siCdc2**	MALDI-TOF MS (calcd)	MALDI-TOF MS (found)
siCdc-2-A	5′-UCGGGAAAUUUCUCUAUUA tt-3′		
siCdc-2-B	3′-tt AGCCCUUUAAAGAGAUAAU-5′		
A strand modification			
RNA-2-A	5′-UCGGGAAAU***isoT$_1$***UCUCUAUUA tt-3′	6616.92	6616.93
RNA-3-A	5′-UCGGGAAAUUUCUCUAU***isoT$_1$***A tt-3′	6616.92	6616.00
B strand modification			
RNA-4-B	3′-tt AGCCCUUU***isoA$_1$***AAGAGAUAAU-5′	6671.98	6672.39
RNA-5-B	3′-tt AGCCCUUUA***isoA$_1$***AGAGAUAAU-5′	6671.98	6671.48
RNA-6-B	3′-tt AGCCCUUUA***isoA$_2$***AGAGAUAAU-5′	6729.00	6730.53
RNA-7-B	3′-tt AGCCCUUU***isoA$_2$***AAGAGAUAAU-5′	6729.00	6729.66

Table 3 T_m values of duplex and calculated free energy (G) of DNA/RNA by computer simulation

DNA/DNA duplex	T_m (°C) DNA/DNA	ΔT_m (°C) [a]	DNA/RNA duplex	T_m (°C) DNA/RNA	ΔT_m (°C) [b] DNA/RNA	G (kcal/mol) DNA/RNA
I/VIII	68.0	–	**I/IX**	76.0	–	–55.45
II/VIII	62.2	–5.8	**II/IX**	71.0	–5.0	–44.76
III/VIII	64.1	–3.9	**III/IX**	70.8	–5.2	–49.55
IV/VIII	64.1	–3.9	**IV/IX**	71.6	–4.4	–54.12
V/VIII	60.1	–7.9	**V/IX**	72.5	**–3.5**	–46.52
VI/VIII	63.1	–4.9	**VI/IX**	72.5	**–3.5**	–45.27
VII/VIII	63.0	–5.0	**VII/IX**	72.5	**–3.5**	–51.60
c-DNA (**VIII**) 3′-TGT AGA GGG CGT AGG GTG AG-5′						
c-RNA (**IX**) 3′-UGU AGA GGG CGU AGG GUG AG-5′						

a) Compare to T_m value (68.0 °C) of **I/VIII** duplex; b) compare to T_m value (76.0 °C) of **I/IX** duplex.

3.5 Circular dichroism

To further confirm the conformations of the hybrid duplexes formed from **II–VII** with their complementary **VIII**, the circular dichroism (CD) spectra were performed (Figure 3). The results showed that the modified duplexes (**II/VIII–VII/VIII**) possessed very similar conformations to that of **I/VIII**, i.e. the standard B-form helix. Although the presence of one incorporated amino-isonucleotide **isoA$_1$** or **isoA$_2$** twisted the backbone, the global conformation could not be significantly affected.

3.6 Computer simulations for DNA/RNA duplexes

The hydrogen bonding was broken at the position of isonucleoside in **V/IX** and **VI/IX**, but the one in **VII/IX** wasn't. The amide at the 6-position of the sugar ring in **isoA$_2$** was involved in the formation of the hydrogen bonding at the position of isonucleoside in **VII/IX**. The reason is that self-regulation releases torsion strain of duplex, resulting in a lower free energy in **VII/IX**.

Both **isoA$_1$** inserted ASONs (**II–IV**) can form intact hydrogen bonding with **IX** (Figure 4). But in **isoA$_2$** inserted ones (**V–VII**), different phenomena were observed (Figure 5). Compared to **VII/IX**, the hydrogen bonding was broken at the position of isonucleoside in **V/IX**, **VI/IX**. This could be the reason why **V/IX** and **VI/IX** have a higher free energy than **VII/IX**, although their T_m values are the same, as perhaps the amide at the 6-position of the sugar ring in **isoA$_2$** is involved in the formation of the hydrogen bonding at the position of isonucleoside. This may be due to the self regulation that releases torsion strain of duplex.

3.7 RNAi potency of siRNAs

To evaluate the influences on the gene silencing efficiencies of both strands of amino-isonucleoside modified siRNA, two mRNA targets were constructed for the both strands of **siCdc2** via siQuant vector, respectively. Each strand of **siCdc2** is considerably active toward its target mRNA in the artificial RNAi assay model, in which an mRNA fragment, perfectly matching the **A** strand or **B** strand of **siCdc2**, was

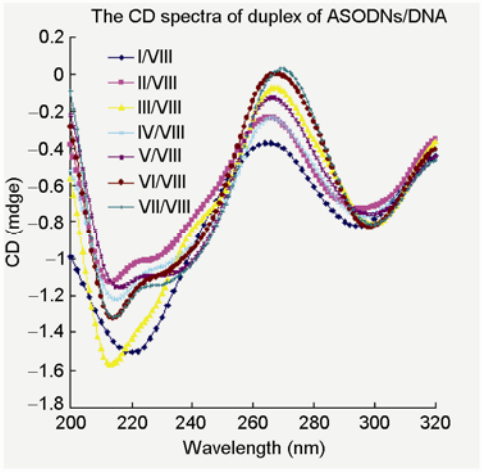

DNA Duplex	Positive cotton peak (nm)	Negative cotton peak (nm)
I/VIII	264	220
II/VIII	265	213
III/VIII	267	213
IV/VIII	266	215
V/VIII	266	216
VI/VIII	268	213
VII/VIII	270	214

Figure 3 CD spectra of **I–VII** with their complementary DNA **VIII** (nm). CD buffer: 57 mM Tris-HCl (pH 7.5), 57 mM KCl and 1 mM $MgCl_2$.

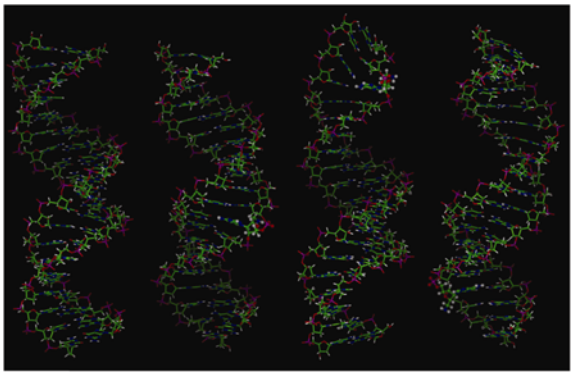

Figure 4 Computer simulated conformation of **I/IX** (first, left), **III/IX** (second, left), **II/IX** (second, right) and **IV/IX** (first, right).

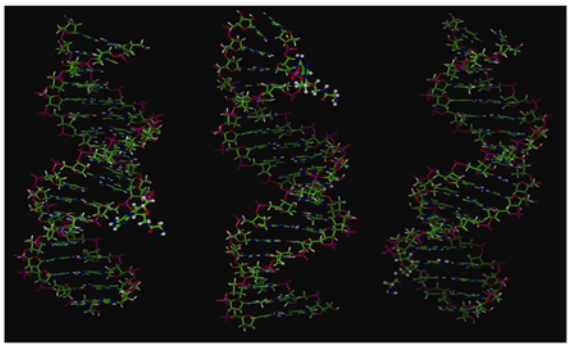

Figure 5 Computer simulated conformation of **VI/IX** (left), **V/IX** (middle) and **VII/IX** (right). The hydrogen bonding was substituted by amide group at the position of **isoA2** in **V/IX**, **VI/IX**.

fused in-frame with the firefly luciferase gene in a mammalian expression vector [19]. The resulting fusion reporter was then used as an artificial target. The **siCdc2** (**siRNA-1**) and **siRNA-2–siRNA-7** were examined for their silencing efficacy on the two targets (Figures 6 and 7).

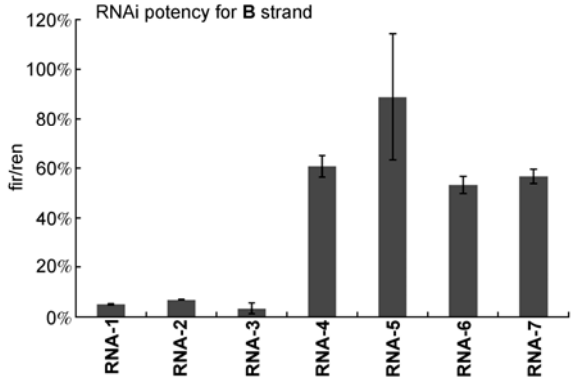

Figure 6 Gene silencing efficiencies of modified **siCdc-2** for **B** strand as guide strand.

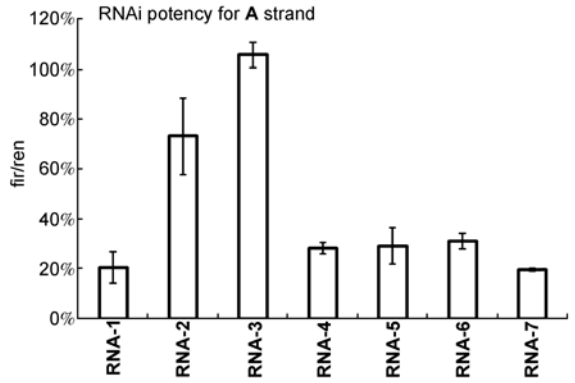

Figure 7 Gene silencing efficiencies of modified **siCdc-2** for **A** strand as guide strand.

We have reported the synthesis of **isoA$_1$** incorporated siRNA, and found that modification on the sense strand retained the silence efficiencies of the siRNA(Wee1) antisense strand [18]. Additionally, the conformation of an ASON was changed at the position of amino-isonucleotide incorporated, which would make the modified ASON less recognized by nucleases and increase its stability toward various enzymes. The thermal stability of modified **siCdc-2** duplex with amino-isonucleoside decreased with lower T_m values. Alternations in torsion angles could promote the passenger strand cleavage or separation from RISC, which could potentially increase silencing efficiency [18]. Here we continued to investigate the RNAi potency of amino-isonucleosides **isoA$_1$**, **isoA$_2$** and **isoT$_1$** incorporated in the middle or 3′-end of siRNA **A** strand or **B** strand. It's known that each strand of the siRNA can be the guide strand, which is loaded into RISC and executes the knockdown effect for the target itself. The gene silencing results of **A** strand will represent the off-target effect by sense strand loading into RISC, and the gene silencing results of **B** strand will represent real RNAi potency of **siCdc-2**. So the artificial assay system is used to investigate this phenomenon.

To investigate the potency of **B** strand, the **A** strand incorporated with **isoT1** in the middle (**RNA-2**) and at the position close to 3′-end (**RNA-3**) were synthesized, respectively. While the former had no influence, the latter slightly increased the silence efficiency of **B** strand. As shown in the Figure 6 the siRNA-3 **B**-strand potency increased slightly. While in the Figure 7, the siRNA-3 **A** strand has no activity. We could image that both strands of siRNA can be loaded into RISC, so there is competition effect between them. Decreasing the activity of one strand may increase the other one. As previously reported, modification incorporated in the middle of **A** strand will inactivate the siRNA (**RNA-4, 5, 6, 7**) [20]. In the process of Ago2 recognition and sense strand release or cleavage, neither of the amino-isonucleoside modifications were suitable substrates for the protein. Because the longer side chain of **isoA$_2$** relieves torsion strain of the duplex (unpublished data), it may slightly enhance the release ability of the sense strand when compared with that of **isoA$_1$** modification. The side chains of the amides (**RNA-6, RNA-7**) have less influence than the amino ones (**RNA-4**, **RNA-5**), although both amino-isonucleoside modifications decreased RNAi potency when incorporated in the middle of the **B** strands (Figure 6, Table 4).

In the previous reports, the 3′-end of the sense strand modified by 2′-OMe nucleosides and many others maintained the silencing efficiencies of siRNAs [21]. Our results show that the overall influence on the RNAi efficiency of

Table 4 The gene silencing activities of **siCdc-2** and amino-isonucleoside modified analogues

No.	**siCdc-2**	Modified position	Silencing efficiencies of **B** strand (%)	Silencing efficiencies of **A** strand (%)
RNA-1	**A**: 5′-UCG GGA AAU UUC UCU AUU Att-3′ **B**: 3′-tt AGC CCU UUA AAG AGA UAA U-5′		94.80	79.50
RNA-2	5′-UCG GGA AAU ***isoT$_1$***UC UCU AUU Att -3′/**B**	10 (S)	93.10	27.10
RNA-3	5′-UCG GGA AAU UUC UCU AU***isoT$_1$*** Att -3′/**B**	18 (S)	96.50	–5.50
RNA-4	**A**/3′-tt AGC CCU UU***isoA$_1$*** AAG AGA UAA U-5′	11 (As)	39.00	71.60
RNA-5	**A**/3′-tt A GC CCU UUA ***isoA$_1$*** AG AGA UAA U-5′	10 (As)	11.00	70.80
RNA-6	**A**/3′-tt A GC CCU UUA ***isoA$_2$***AG AGA UAA U-5′	10 (As)	46.50	68.90
RNA-7	**A**/3′-tt A GC CCU UU ***isoA$_2$*** AAG AGA UAA U-5′	11 (As)	43.00	80.40

modified **A** strand is similar to that of **B** strand. However, because the original RNAi potency of **A** strand is relatively low, the influence of modifications is more obvious [22]. When **isoT$_1$** was incorporated in the **A** strand at the 18th position, its RNAi efficiency completely disappeared (**RNA-3**) (Figure 7, Table 4). It's reported that the PAZ domain of Ago2 initially binds to the 3′-end of siRNA, and once the target mRNA comes and starts to anneal to the siRNA, the 3′-end of the guide strand is released from it, with the release step being the rate-limiting step in this process [23]. The amino-isonucleosides with greater stereo hindrance than the 2′-OMe nucleosides incorporated near the 3'-end of the guide strand may interrupt the binding or releasing step. The possibility of difficulty in the TRBP or Dicer binding step before the formation of the RISC loading complex (**RLC**) cannot be eliminated, for TRBP binds 3′-half of siRNA and then transfers it to Ago2 to form **RLC** under the help of Dicer. The steric hindrance of isonucleotides may influence protein recognition and binding process in the prior step.

Combined with our previous reports [18], it is concluded that amino-isonucleosides incorporated in the middle, 3′-end or 5′-end of siRNA **A** strand all inhibit the RNAi efficiency of this strand, which means reduction of the off-target effect by sense strand loading into RISC. Additionally, these two reporters can be treated as two independent siRNA targets with different potency. Modification in one strand merely influenced the silencing efficiency of another, which would mean the modifications didn't influence the cleavage or unwinding of the modified passenger strand of siRNA after RISC formation. In fact, it is necessary to modify more other positions of passenger strand of siRNA to give more detailed data to support the conclusion above in the future work. Both strands of siRNA can be loaded into RISC and execute knockdown effect of the corresponding target, which may be due to the competitive effect between **A** strand and **B** strand loading into RISC [24].

4 Conclusion

In this work, we have reported the synthesis of a novel class of amino-isonucleoside **isoA$_2$**. Furthermore, two amino-isonucleosides **isoA$_1$** and **isoA$_2$** were selected to incorporate into the natural ASON **I** to investigate the basic physicochemical properties. The UV melting experiment and the CD spectra showed that individual **isoA$_1$** and **isoA$_2$** modifications slightly affect the stability and conformation of duplexes, and **III** and **VII** were highly resistant to SVPDE, meanwhile **II** was slightly resistant to the exonuclease.

We further incorporated these amino-isonucleosides, including **isoT$_1$**, into a siRNA (**siCdc-2**). Especially when isonucleoside was incorporated at the 3′-end of **A** strand, the RNAi efficiency of **B** strand was slightly increased. Meanwhile, amino-isonucleosides incorporated in the middle, 3′-end or 5′-end of siRNA sense strand all decrease the RNAi potency of this strand. Those results mean that the off-target effect by sense strand loading into RISC could be reduced by sense strand modification with amino-isonucleoside. We have obtained some promising results from amino-isonucleosides incorporation with ASONs or siRNAs, which could make some contributions to further research and therapeutic application.

We thank Prof. LIANG Zi-Cai, DU Quan and YI Fan in Peking University, for providing siRNA sequence and assistance with biological assay experiments. This work was supported by the National Natural Science Foundation of China (20932001), and the Ministry of Science and Technology of China (2006AA02Z144, 2009ZX09503).

Abbreviations

ASONs antisense oligonucleotides
CD circular dichroism
CPG controlled pore glass
DCC dicyclohexyl carbodiimide
DIPEA diisopropylethylamine
DMF dimethyl formide
DMSO dimethylsulfoxide
DMT 4,4′-dimethoxytriphenyl
EDTA ethylenediamine tetraacetic acid
ESI-TOF electrospray ionization-time of flight
HRMS high resolution mass spectrometry
HPLC high performance liquid chromatography
MALDI matrix-assisted laser desorption ionization
MS mass spectrometry
PNA peptide nucleic acid
PS-ASONs phosphorothioates antisense oligonucleotides
^{31}P NMR phosphorus-31 nuclear magnetic resonance
Py pyridine
RNAi RNA interference
RISC RNA induced silencing complex
RLC RISC loading complex
SVPDE snake venom phosphodiesterase
TEAB triethyl-ammonium bicarbonate
TFA trifluoroacetyl
THF tetrahydrofuran
TIP3P transferable intermolecular potential (function) 3 points
T_m temperature of melting
TMSCl trimethylsilyl chloride
TOF time of flying

1 Kathleen FP, Antonina R, Leanne SS, Esther HC. Antisense therapeutics: From theory to clinical practice. *Pharmac Therap*, 2003, 99: 55–77
2 Kim DH, Rossi JJ. Overview of gene silencing by RNA interference. *Curr Protoc Nucleic Acid Chem*, 2009. Chapter 16. Unit 16.1
3 Elbashir SM, Harborth J, Lendeckel W, Yalcin A, Weber K, Tuschl T.

Duplexes of 21-nucleotide RNAs mediate RNA interference in cultured mammalian cells. *Nature*, 2001, 411(6836): 494–498
4 Chiang MY, Chan H, Zounes MA, Freier SM, Lima WF, Bennett CF. Antisense oligonucleotides inhibit intercellular adhesion molecule 1 expression by two distinct mechanisms. *J Biol Chem*, 1991, 266: 18162–18171
5 Crooke ST. Oligonucleotide therapeutics. In: *Burger's Medicinal Chemistry and Drug Discovery*. Vol. 1: Principles and Practice. Wolff ME, Ed. John WS, Inc., New York, 1995. 863–900
6 Crooke ST. Oligonucleotide therapy. *Curr Opin Biotechnol*, 1992, 3: 656–661
7 Pushparaj PN, Aarthi JJ, Manikandan J, Kumar SD. siRNA, miRNA, and shRNA: *In vivo* applications. *J Dent Res*, 2008, 87(11): 992–1003
8 Whitehead KA, Langer R, Anderson DG. Knocking down barriers: Advances in siRNA delivery. *Nat Rev Drug Discov,* 2009, 8(2): 129–138
9 Wullner U, Neef I, Tur MK, Barth S. Targeted delivery of short interfering RNAs–strategies for *in vivo* delivery. *Rec Patents Anti Can Drug Disc,* 2009, 4(1): 1–8
10 Yang ZJ, Yu HW, Min JM, Ma LT, Zhang LH. Stereoselective synthesis of 4-deoxy-4-nucleobase-2,5-anhydro-L-mannitol derivatives. *Tetrahedron Asymm*, 1997, 8: 2739–2747
11 Wang JF, Yang XD, Zhang LR., Yang ZJ, Zhang LH. Synthesis and biological activities of 5′-ethylenic and acetylenic modified L-nucleosides and isonucleosides. *Tetrahedron*, 2004, 60: 8535–8546
12 Yu HW, Zhang LR, Zhou JC, Ma LT, Zhang LH. Studies on the synthesis and biological activities of 4′-(*R*)-hydroxy-5′-(*S*)-hydroxymethyltetrahydrofuranyl purines and pyrimidines. *Bioorg Med Chem*, 1996, 4: 609–614
13 Jiang CW, Li BC, Guan Z, Yang ZJ, Zhang LR, Zhang LH. Synthesis and recognition of novel isonucleoside triphosphates by DNA polymerases. *Bioorg Med Chem*, 2007, 15: 3019–3025
14 Lei Z, Min JM, Zhang LH. Synthesis of 3-deoxy-3-nucleobase-2,5-anhydro-D-mannitol: A novel class of hydroxymethyl-branched isonucleosides. *Tetrahedron Asymm*, 2000, 11: 2899–2906
15 Wang ZL, Shi JF, Jin HW, Zhang LR, Lu JF, Zhang LH. Properties of isonucleotide-incorporated oligodeoxynucleotides and inhibition of the expression of spike protein of SARS-CoV. *Bioconj Chem*, 2005, 16: 1081–1087
16 Bernard C, Florence C, Dieter H, François N, Romain MW, Karl-Heinz A, Pierre M, Heinz EM. Dual recognition of double-stranded DNA by 2'-aminoethoxy-modified oligonucleotides. A*ngew Chem Int Ed*, 1998, 37: 1288–1291
17 Massey PA, Sigurdsson TS. Chemical syntheses of inhibitory substrates of the RNA-RNA ligation reaction catalyzed by the hairpin ribozyme. *Nucleic Acids Res*, 2004, 32: 2017–2022
18 Li ZS, Qiao RP, Du Q, Yang ZJ, Zhang LR, Zhang PZ, Liang ZC, Zhang LH. Studies on aminoisonucleoside modified siRNAs: stability and silencing activity. *Bioconjug Chem*, 2007, 18(4): 1017–1024
19 Du Q, Thonberg H, Zhang HY, Wahlestedt C, Liang ZC. Validating siRNA using a reporter made from synthetic DNA oligonucleotides. *Biochem Biophys Res Commun*, 2004, 325(1): 243–249
20 Matranga C, Tomari Y, Shin C, Barte DP, Zamore PD. Passenger-strand cleavage facilitates assembly of siRNA into Ago2-containing RNAi enzyme complexes. *Cell*, 2005, 123(4): 607–620
21 Kurreck J. RNA Interference: From basic research to therapeutic applications. A*ngew Chem Int Ed*, 2009, 48(8): 1378–1398
22 Wei JX, Yang J, Sun JF, Jia LT, Zhang Y, Zhang HZ, Li X, Meng YL, Yao LB, Yang AG. Both strands of siRNA have potential to guide posttranscriptional gene silencing in mammalian cells. *PLoS One*, 2009, 4(4): e5382
23 Li F, Pallan PS, Maier MA, Rajeev KG, Mathieu SL, Kreutz C, Fan YP, Sanghvi J, Ronald M, Rozners E, Manoharan M, Egli M. Crystal structure, stability and *in vitro* RNAi activity of oligoribonucleotides containing the ribo-difluorotoluyl nucleotide: insights into substrate requirements by the human RISC Ago2 enzyme. *Nucleic Acids Res*, 2007, 35(19): 6424–6438
24 Clark PR, Pober JS, Kluger MS. Knockdown of TNFR1 by the sense strand of an ICAM-1 siRNA: Dissection of an off-target effect. *Nucleic Acids Res*, 2008. 36(4): 1081–1097